

A Novel Switching Sequence For Multi-Terminal Phase Shift SRI For Induction Heating Applications

1. V.PRABHAVATHI, PG Student, 2. C. Balachandra Reddy, Professor & HOD
Department of EEE, CBTVIT, Hyderabad

Abstract - The purpose of this work was the development of an IGBT PS full-bridge inverter of 100 kW and 50 kHz where the switching sequence was modified in order to improve its reliability in industrial applications like induction heating where a large number of cycles are required. The modified PS inverter is a cost-effective solution that incorporates the following improvements. Home appliances represent a substantial part of the residential energy consumption. For this reason the efficiency of the power converter is a key design aspect, as it defines not only the environmental impact but also the final appliance performance and reliability. This paper describes an induction heating system of 100 kW and 50 kHz for industrial applications, which uses a novel control scheme based on a PS IGBT full-bridge SRI that allows us to improve its reliability significantly by increasing the lifetime of the IGBTs. To achieve this, the inverter should always perform zero-voltage switching (ZVS) operation and the impact of the turn-off switching losses in the temperature increase of the IGBT junction should be as low as possible.

I. INTRODUCTION

Home appliances represent a substantial part of the residential energy consumption. For this reason the efficiency of the power converter is a key design aspect, as it defines not only the environmental impact but also the final appliance performance and reliability. As a consequence, researches and developments on induction cookers, as one of the more consuming appliances, pursue further efficiency improvements.

Domestic induction heating technology has become more important in recent years due to advantages such as its improved efficiency, safety and performance. The main blocks of an induction cooking appliance are outlined in Fig. 1. The mains voltage is rectified and filtered, generating a DC bus. Afterwards, the resonant inverter supplies variable frequency current (20 to 75 kHz) to the induction coil. This current produces an alternating magnetic field, which causes eddy currents and magnetic hysteresis heating up the pan.

Traditional Square Wave (SW) modulation implies operation at high switching frequencies to deliver low-medium power. This entails inverter efficiency reductions, which is a basic fact to ensure reliability,

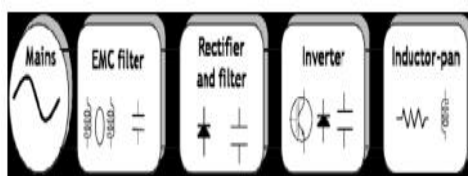


Fig. 1. Block diagram of a domestic induction cooking appliance

Maximize output power capabilities and minimize heat sink and fan size. In the past, Pulse Density Modulation has been proposed to improve the efficiency. However, it has some limitations regarding flicker emissions and user performance.

The aim of this paper is to propose a control algorithm optimization leading to an efficiency improvement with no hardware changes required. To achieve this goal, a theoretical analysis of Variable Frequency Duty Cycle (VFDC) modulation scheme has been carried out. Afterwards, efficiency obtained at different operation conditions has been estimated for different switching devices. Finally, experimentation with a typical induction heating inverter has been used to validate the simulation results.

Induction heating generators are resonant inverters in which the resonant tank is formed by the heating coil and a capacitor in a series resonant inverter (SRI) [1] or in a parallel resonant inverter (PRI) [2]. They are used to heat metals to be welded, melted, or hardened. The use of SRIs that are fed with a voltage source represents a cost-effective solution. In order to regulate the output power, using a diode bridge rectifier as a dc voltage source, inverters with power control by frequency (FC) [3], phase-shift (PS) variation [4], [5], or pulse density modulation (PDM) [6], [7] are normally used.

These power control schemes, however, may result in an increase of switching losses and electromagnetic noise because it is impossible for switching devices to be always turned on and off under zero-current condition. Therefore, in high-frequency induction heating applications, only MOSFET inverters can be used. Nevertheless, isolated-gate bipolar transistors (IGBTs) are preferred in high-power industrial applications (availability, cost, etc.), and it will only be possible if a low-loss power control scheme is found. Induction heating applications, particularly induction hardening, are repetitive processes with relatively low periods. This means that an induction heating inverter can make several cycles per minute. Under these conditions, the IGBT power cycling capability is one of the most important reliability items that relates directly to the lifetime of the inverter. Since the failure mechanism depends on the IGBT T_j , we can improve the inverter reliability reducing the transistor losses or improving the thermal management [8].

This paper describes an induction heating system of 100 kW and 50 kHz for industrial applications, which uses a novel control scheme based on a PS IGBT full-bridge SRI that allows us to improve its reliability significantly by increasing the lifetime of the IGBTs. To achieve this, the inverter should always perform zero-voltage switching (ZVS) operation and the impact of the turn-off switching losses in the temperature increase of the IGBT junction should be as low as possible. The inverter working frequency is automatically adjusted close to the resonance frequency in order to allow a quasi-zero-current switching inverter operation of one leg of the inverter for any load condition. The blanking time of the inverter transistors is designed to maintain ZVS mode [7]. Additionally, an appropriate switching sequence for the PS control of the inverter allows the reduction of the T_j of the IGBTs of the other leg of the inverter.

This paper is organized as follows. Section II shows the configuration of the inverter, and Section III analyzes the basic operation and main parameters of the inverter. Section IV describes the new inverter switching sequence and the control strategy and gives relevant simulation results. Section V validates the simulation results using experimental data, and Section VI makes a comparative study between the proposed and the standard PS power control. Finally, the conclusions are drawn.

II. LITERATURE SURVEY

Fig 2.2 shows the idealized schematic diagram of the inverter circuit where the transformer $T1$ has been removed and, hence, the impedances have been transformed by the turns ratio $n1$. $Q1-Q4$ and $D1-D4$ are, respectively, the IGBT transistors and the free-wheeling diodes that compose each power module.

$C1-C4$ represent the equivalent capacitance of the inverter switches, including the snubbing capacitor and the output capacitance of the IGBTs. We will suppose that all these capacitances have the same value C_S .

The simplified output voltage and current waveforms of the inverter are represented in Fig 2.3. The four transistors $Q1-Q4$ are operated with almost a 50% duty cycle. The switches in each leg of the bridge are turned on and off approximately (except the blank time) 180° out of phase. It operates above resonance, and the load current i_o lags the quasi-square wave voltage v_o , as shown in Fig 2.3. Free-wheeling diodes conduct current after C_S is discharged. During this diode conduction period, the IGBTs can be turned on at zero voltage. $Q1$ and $Q2$ are the main leg transistors of the inverter that switch on and off near to the zero crossing of the output current. The output power of the inverter is regulated by varying the PS between switches $Q1$ and $Q3$ (or $Q2$ and $Q4$). The resulting voltage across the resonant circuit is a quasi-square wave clamped at zero during the time corresponding to the PS. The power module current (diode and transistor) of the main leg and the phase-shifted leg are i_{QD1} and i_{QD3} , respectively. Note that only i_{QD3} presents a high value of the switching current i_C (collector current being turned off).

We call v_o the voltage between points a and b (Fig 2.2). It represents the output voltage of the inverter,

and v_1 is its corresponding first harmonic whose amplitude is

$$V_1 = \frac{4V_d}{\pi} \cos \frac{\varphi}{2} \quad (1)$$

where V_d is the average value of the dc-link voltage.

The phase between the output current and output voltage and, hence, the phase of the resonant circuit impedance at the working frequency is α , and the module of this impedance can be expressed by

$$|Z(j\omega)| = \left| R + jL\omega + \frac{1}{jC\omega} \right| = \frac{R}{\cos \alpha} \quad (2)$$

As the value of α is approximately equal to $\pi/2$, then the amplitude of the output current is given by

$$I_o = \frac{4V_d}{\pi R} \cos^2 \frac{\varphi}{2} \quad (3)$$

Therefore, the output power is

$$P = \left(\frac{I_o}{\sqrt{2}} \right)^2 R = \frac{8V_d^2}{\pi^2 R} \cos^4 \frac{\varphi}{2} \quad (4)$$

The phase portion α , where the output voltage is increasing from zero to positive and the output current is negative, is essential to determine the ZVS operation. A mathematical expression for the minimum values of α required to achieve ZVS is obtained from the following charge analysis [6]: The current in the resonant circuit must be large enough to change the voltage in the switching capacitor C_S up to V_d (or $-V_d$) in the time t_{min} just before the output current crosses zero.

From these charge relations, t_{min} can be calculated as

$$\beta_{min} = \cos^{-1} \left(1 - \frac{2\omega_o C_S V_d}{I} \right) \quad (5)$$

The phase β_{min} determines the minimum blank time between the transistors of the main leg of the inverter. The blank time must be calculated continuously using (5) with enough safety margin. In practice, we adjust $\beta = 1.1 \text{ min}$. On the other hand, the PS regulation implies a change of switching frequency ω above the resonant frequency ω_o as a function of PS angle, as shown in the following [7]:

$$\omega = \omega_o \frac{\tan \frac{\varphi}{2} + \sqrt{\tan^2 \frac{\varphi}{2} + 4Q^2}}{2Q} \quad (6)$$

where Q is the quality factor of the series resonant circuit

$$\omega_o = \frac{1}{\sqrt{LC}} \quad Q = \frac{L\omega_o}{R} \quad (7)$$

We can calculate the conduction losses of the transistor and the diodes of the inverter using a linear approximation of its direct characteristic. This means that the relations between the device drop voltage and current (v_F and i_F for the diode and v_{CE} and i_C for the transistor) are

$$v_F = k_1 i_F + k_2 \quad \text{and} \quad v_{CE} = k_3 i_C + k_4 \quad (8)$$

For the power device used in our inverter, the values of the constants are

$$k_1 = 0.0017 \quad k_2 = 0.8 \text{ V}$$

$k_3 = 0.004$
 $k_4 = 1.6 \text{ V}$.

Under these conditions, we can obtain the conduction power losses of the diode as

$$P_{CD} = \frac{I_o}{2\pi} \left[k_1 \frac{I_o}{2} \left(\delta - \frac{\sin 2\delta}{2} \right) + k_2(1 - \cos \delta) \right] \tag{9}$$

and transistor conduction losses can be expressed as

$$P_{CT} = \frac{I_o}{2\pi} \left[k_3 \frac{I_o}{2} \left(\pi - \delta + \frac{\sin 2\delta}{2} \right) + k_4(1 + \cos \delta) \right] \tag{10}$$

where δ is equal to δ_1 for the transistors of the main leg of the inverter and δ_2 is equal to δ_2 for the transistors of the other leg.

Switching losses must be also computed. Considering that there are no significant losses in the switching process of the diodes and that the ZVS operation of the transistor is allowed, the only switching losses correspond to the turn-off of the IGBTs. In this situation, the switching losses can be calculated by the following:

$$P_{ST} = f E_{off} \tag{11}$$

where f is the inverter switching frequency and E_{off} denotes the turn-off energy losses of the IGBT. The manufacturer of the transistor gives in the data sheets of the device the characteristic curve of E_{off} as a function of the switching current I_C . If we liberalize this curve, we can give a simple expression for calculating the switching power losses

$$P_{ST} = f(k_5 I_C + k_6) \tag{12}$$

where, for our transistor, the constants are

$$k_5 = 0.0664 \text{ V} \cdot \text{s}$$

$$k_6 = 1.75 \text{ W} \cdot \text{s}$$

Fig 3.1. Power losses of the transistor of the inverter versus output power.

The switching current of the inverter transistor I_C is

$$I_C = \frac{4V_d}{\pi R} \cos^2 \frac{\varphi}{2} \sin \delta \tag{13}$$

where δ is equal to δ_1 for the transistors of the main leg of the inverter and δ_2 is equal to δ_2 for the transistors of the other leg.

Figure 3.1 shows the results of the calculation of the conduction and switching losses for one of the four IGBT transistors of the inverter obtained by (10) and (12). P_{CQ1Q2} represents the conduction power losses of one of the transistors of the main leg ($Q1$ or $Q2$), P_{CQ3Q4} represents the conduction power losses of one of the transistors of the phaseshifted leg ($Q3$ or $Q4$), P_{SQ1Q2} represents the switching power losses of one of the transistors of the main leg ($Q1$ or $Q2$), and P_{SQ3Q4} represents the switching power losses of one of the transistors of the phase-shifted leg ($Q3$ or $Q4$). Note that the power switching losses of these last transistors, calculated by (12), increase when the output power regulation decreases due to two factors: the increase of the

switching current I_C given by (13) and the increase of the working frequency given by (6).

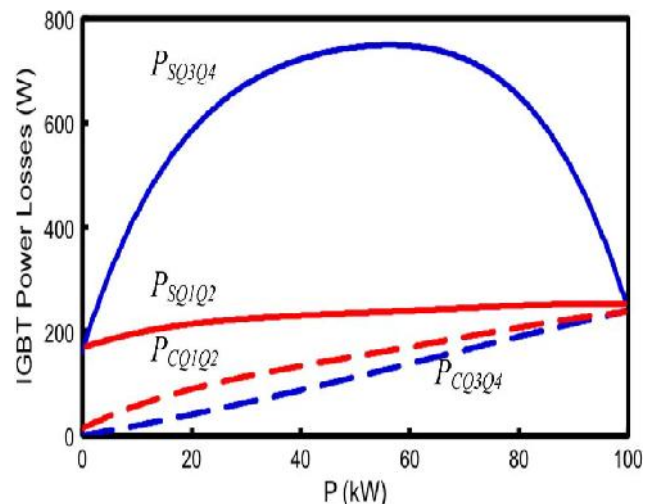
III. PROPOSED METHOD AND RESULTS

Power electronics refers to control and conversion of electrical power by power semiconductor devices wherein these devices operate as switches. Advent of silicon-controlled rectifiers, abbreviated as SCRs, led to the development of a new area of application called the power electronics. Prior to the introduction of SCRs, mercury-arc rectifiers were used for controlling electrical power, but such rectifier circuits were part of industrial electronics and the scope for applications of mercury-arc rectifiers was limited. Once the SCRs were available, the application area spread to many fields such as drives, power supplies, aviation electronics, high frequency inverters and power electronics originated. Electronic power converter is the term that is used to refer to a power electronic circuit that converts voltage and current from one form to another. These converters can be classified as:

- Rectifier converting an ac voltage to a dc voltage,
- Inverter converting a dc voltage to an ac voltage,
- Chopper or a switch-mode power supply that converts a dc voltage to another dc voltage.
- Cycloconverter converting an ac voltage to another ac voltage.

Single phase DC-AC inverter:

A single-phase square wave type voltage source inverter produces square shaped output voltage for a single-phase load. Such inverters have very simple control logic and the power switches need to operate at much lower frequencies compared to switches in some other types of inverters. The first generation inverters, using thyristor switches, were almost invariably square wave inverters because thyristor switches could be switched on and off



only a few hundred times in a second. In contrast, the present day switches like IGBTs are much faster and used at switching frequencies of several kilohertz.

Resonant converters:

Resonant inverters are electrical inverters based on resonant current oscillation. In series resonant inverters the resonating components and switching device are placed in series with the load to form an underdamped

circuit. The current through the switching devices fall to zero due to the natural characteristics of the circuit. If the switching element is a thyristor, it is said to be self-commutated.

Role of current ripple reduction in PWM inverters:

The inverter switches need to be rated to withstand the peak magnitude of input dc link voltage, the maximum expected load current and should be able to safely dissipate the heat generated in the switch due to conduction and switching losses. Because of high frequency switching, the switches in PWM inverters have significantly more switching loss. Often the switch chosen in PWM inverters is oversized, in terms of its current rating, so that the sum total of switching loss and conduction loss remains well within the heat dissipation capability of the switch and the associated heat sink. Constant switching frequency PWM method gives benefits for design and implementation of the converters, but fails to address the problems in three phase converters. Current ripple and Electromagnetic interference (EMI) is not justified using constant frequency switching PWM technique.

So to overcome the above problem in this project variable switching frequency PWM technique is proposed to overcome different current ripple problems.

Literature survey:

According to Akira Morozumi, Katsumi Yamada, Tadashi Miyasaka, Sachio Sumi, and Yasukazu Seki, Power cycling capability is one of the most important reliability items in the application of power semiconductor modules. This paper describes the failure mechanism of power cycling by analysis of the structure of lead-based solder and joint failure due to solder fatigue. By the application of some additional elements, it has been found that a newly developed tin-silver-based solder shows both excellent mechanical properties and wettability. Further, we have established, both by experiment and computer calculation, that the dependence of the failure mechanism on θ is completely different between the new tin-silver-based solder and conventional lead-based solder.

According to A. Suresh and S. Rama Reddy, Resonant converters find a very wide application in Induction heating, which requires high frequency currents. Series and Parallel resonant inverters are employed for this purpose. This paper gives a comparative analysis of series and parallel resonant inverter fed ferromagnetic load based on experiments carried out and finally concluded which is the suitable inverter for Induction heating application, whether it is Series Resonant Inverter (SRI) or Parallel Resonant Inverter (PRI) based on the experimental results. The results of SRI are compared with that of PRI and presented.

According to François Forest, Sébastien Faucher, Jean-Yves Gaspard, Didier Montloup, Jean-Jacques Huselstein, and Charles Joubert The induction heating principle has been successfully introduced for about 20 years in domestic cooking appliances. The technical developments now concern the improvement of the current appliances and the introduction of new functions. So, one tendency is the design of multiwinding induction coils that are very adaptive concerning the shape and the power capability. This paper describes different original

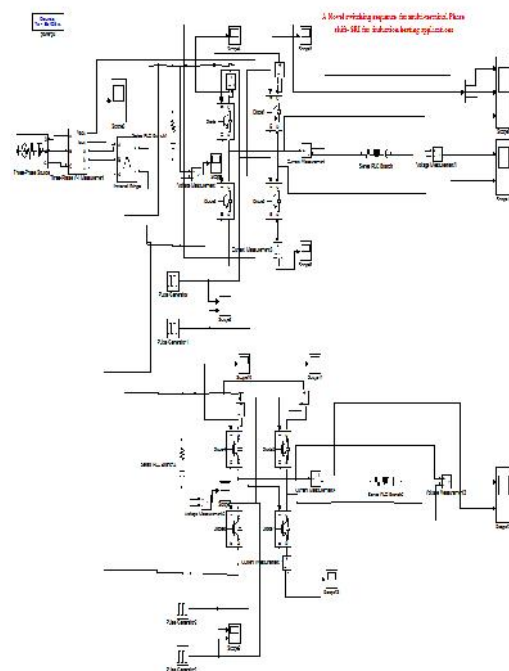
converter topologies designed to supply multiwinding coils, and, in addition, multicoil systems. The proposed topologies are based on particular use and associations of zero-voltage switching series-resonant converters.

The aim of this project is design the simple neutral point potential (NPP) regulator for a three-level diode-clamped inverter employing a sine-triangle regulator in conjunction with a closed-loop controller with reduced switching losses.

Proposed method:

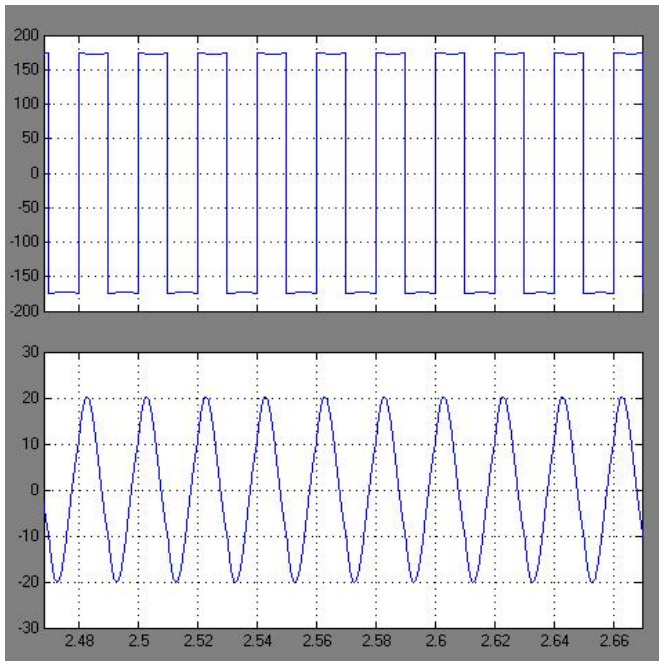
In this system we discussed PS IGBT full-bridge SRI that allows us to improve its reliability significantly by increasing the lifetime of the IGBTs. To achieve this, the inverter should always perform zero-voltage switching (ZVS) operation and the impact of the turn-off switching losses in the temperature increase of the IGBT junction should be as low as possible. The inverter working frequency is automatically adjusted close to the resonance frequency in order to allow a quasi-zero-current switching inverter operation of one leg of the inverter for any load condition.

Simulink model

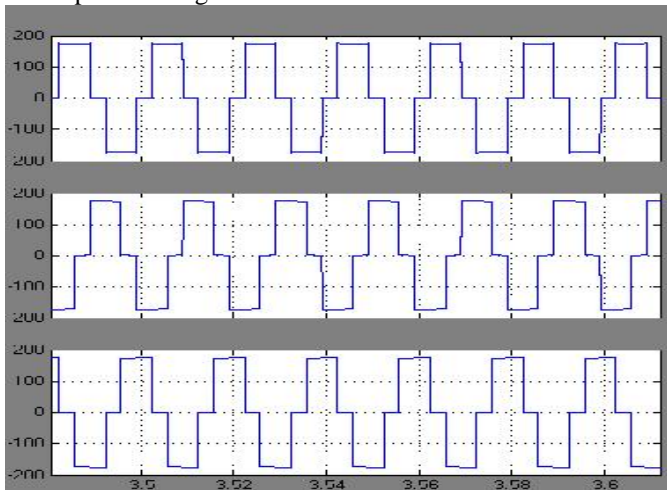


Improving the Reliability of SRI for Induction Heating Applications

Output voltage and current



Three phase voltage



CONCLUSION

The purpose of this work was the development of an IGBT PS full-bridge inverter of 100 kW and 50 kHz where the switching sequence was modified in order to improve its reliability in industrial applications like induction heating where a large number of cycles are required. The modified PS inverter is a cost-effective solution that incorporates the following improvements.

1. The output power is regulated by varying the PS between the switches that compose the legs of the inverter.
2. The control circuit was designed to perform ZVS under all operating conditions.
3. The increment of temperature of the IGBT's junctions was minimized by the use of a novel switching sequence of the transistors.
4. The power cycling capability of the inverter was significantly improved in comparison with the standard PS inverter.

5. The lifetime of the inverter can be incremented for applications of a large number of cycles like induction hardening and others.

Comparing the experimental and simulated results, the validity of the proposed inverter has been demonstrated

REFERENCES

- [1] S. Faucher, F. Forest, J.-Y. Gaspard, J.-J. Huselstein, C. Joubert, and D. Montloup, "Frequency-synchronized resonant converters for the supply of multiwinding coils in induction cooking appliances," *IEEE Trans. Ind. Electron.*, vol. 54, no. 1, pp. 441–452, Feb. 2007.
- [2] A. Shenkman, B. Axelrod, and V. Chudnovsky, "Assuring continuous input current using a smoothing reactor in a thyristor frequency converter for induction metal melting and heating applications," *IEEE Trans. Ind. Electron.*, vol. 48, no. 6, pp. 1290–1292, Dec. 2001.
- [3] L. A. Barragán, D. Navarro, J. Acero, I. Urriza, and J. M. Burdio, "FPGA implementation of a switching frequency modulation circuit for EMI reduction in resonant inverters for induction heating appliances," *IEEE Trans. Ind. Electron.*, vol. 55, no. 1, pp. 11–20, Jan. 2008.
- [4] H. Sarnago, O. Lucia, A. Mediano, and J.M. Burdio, "Modulation scheme for improved operation of an RB-IGBT-based resonant inverter applied to domestic induction heating," *IEEE Trans. Ind. Electron.*, vol. 60, no. 5, pp. 2066–2073, May 2013.
- [5] C. A. F. Ferreira and B. V. Borges, "Sine-wave amplitude-modulation concept for linear behavior of phase-modulated resonant converters," *IEEE Trans. Ind. Electron.*, vol. 60, no. 5, pp. 2074–2083, May 2013.
- [6] V. Esteve, E. Sanchis-Kilders, J. Jordan, E. J. Dede, C. Cases, E. Maset, J. B. Ejea, and A. Ferreres, "Improving the efficiency of IGBT seriesresonant inverters using pulse density modulation," *IEEE Trans. Ind. Electron.*, vol. 58, no. 3, pp. 979–987, Mar. 2011.
- [7] H. Fujita and H. Akagi, "Pulse-density-modulated power control of a 4 kW450 kHz voltage-source inverter for induction melting applications," *IEEE Trans. Ind. Appl.*, vol. 32, no. 2, pp. 279–286, Mar./Apr. 1996.
- [8] A. Morozumi, K. Yamada, T. Miyasaka, S. Sumi, and Y. Seki, "Reliability of power cycling for IGBT power semiconductor modules," *IEEE Trans. Ind. Appl.*, vol. 39, no. 3, pp. 665–671, May/Jun. 2003.
- [9] J. Acero, O. Lucia, I. Millan, L. A. Barragan, J. M. Burdio, and R. Alonso, "Identification of the material properties used in domestic induction heating appliances for system-level simulation and design purposes," in *Proc. APEC*, 2010, pp. 439–443.
- [10] S. Chudjuarjeen, A. Sangswang, and C. Koopai, "An improved LLC resonant inverter for induction-heating applications with asymmetrical control," *IEEE Trans. Ind. Electron.*, vol. 58, no. 7, pp. 2915–2925, Jul. 2011.
- [11] Y.-K. Lo, C.-Y. Lin, M.-T. Hsieh, and C.-Y. Lin, "Phase-shifted full-bridge series-resonant DC-DC converters for wide load variations," *IEEE Trans. Ind. Electron.*, vol. 58, no. 6, pp. 2572–2575, Jun. 2011.
- [12] O. Lucia, J. M. Burdio, L. A. Barragan, C. Carretero, and J. Acero, "Series resonant multiinverter with discontinuous-mode control for improved light-load operation," *IEEE Trans. Ind. Electron.*, vol. 58, no. 11, pp. 5163–5171, Nov. 2011.
- [13] X. Sun and M. Cheng, "Thermal analysis and cooling system design of dual mechanical port machine for wind power application," *IEEE Trans. Ind. Electron.*, vol. 60, no. 5, pp. 1724–1733, May 2013.
- [14] M. Schulz, "Designed to last—Electrical and thermal aspects in power electronic designs," in *Proc. IEEE ICIT*, 2013, pp. 499–502.